AD-752 4[illegible]0

STUDY OF THE FACTORS WHICH AFFECT THE ADEQUACY OF HIGH-STRENGTH, LOW ALLOY STEEL WELDMENTS FOR CARGO SHIP HULLS

E. B. Norris, et al

Southwest Research Institute

Prepared for:

Naval Ship Systems Command

1972

SSC-232

STUDY OF THE FACTORS WHICH AFFECT THE ADEQUACY OF HIGH-STRENGTH, LOW-ALLOY STEEL WELDMENTS FOR CARGO SHIP HULLS

SHIP STRUCTURE COMMITTEE

1972

SHIP STRUCTURE COMMITTEE

AN INTERAGENCY ADVISORY
COMMITTEE DEDICATED TO IMPROVING
THE STRUCTURE OF SHIPS

MEMBER AGENCIES:

UNITED STATES COAST GUARD
NAVAL SHIP SYSTEMS COMMAND
MILITARY SEALIFT COMMAND
MARITIME ADMINISTRATION
AMERICAN BUREAU OF SHIPPING

ADDRESS CORRESPONDENCE TO

SECRETARY
SHIP STRUCTURE COMMITTEE
U.S. COAST GUARD HEADQUARTERS
WASHINGTON, D.C. 20591

SR-177
1972

Dear Sir:

Development of information for use in selection of steels for ships' hulls has been a primary purpose of the Ship Structure Committee since its beginning. Accordingly, appropriate research was initiated early in the development of the high-strength, low-alloy structural steels and several Ship Structure Committee reports have been issued on this subject.

This report contains further information on this research, discussing the properties of these steels both as they come from the mill and after simulated shipyard fabrication.

Comments on this report would be welcomed.

Sincerely,

W. F. REA, III
Rear Admiral, U. S. Coast Guard
Chairman, Ship Structure Committee

UNCLASSIFIED

Security Classification

DOCUMENT CONTROL DATA - R & D

(Security classification of title, body of abstract and indexing annotation must be entered when the overall report is classified)

1. ORIGINATING ACTIVITY (Corporate author) Southwest Research Institute San Antonio, Texas	2a. REPORT SECURITY CLASSIFICATION Unclassified 2b. GROUP

3. REPORT TITLE

Study of the Factors Which Affect the Adequacy of High-Strength, Low-Alloy Steel Weldments for Cargo Ship Hulls

4. DESCRIPTIVE NOTES (Type of report and inclusive dates)

5. AUTHOR(S) (First name, middle initial, last name)

E. B. Norris, A. G. Pickett, and R. D. Wylie

6. REPORT DATE	7a. TOTAL NO. OF PAGES	7b. NO. OF REFS
July 1972	36	5

8a. CONTRACT OR GRANT NO. N00024-67-C-5416	9a. ORIGINATOR'S REPORT NUMBER(S)
b. PROJECT NO.	
c.	9b. OTHER REPORT NO(S) (Any other numbers that may be assigned this report) SSC-231
d.	

10. DISTRIBUTION STATEMENT

Unlimited

11. SUPPLEMENTARY NOTES	12. SPONSORING MILITARY ACTIVITY Naval Ship Systems Command

13. ABSTRACT

High-strength, low-alloy quenched and tempered steels of 100,000-psi minimum yield strength are being used in ship hull structures. A project was initiated by the Ship Structure Committee to define which mechanical properties should be used as performance criteria, to evaluate the suitability of these criteria with large-scale test weldments, and to select small-scale laboratory tests that correlate with the large-scale tests. A survey of available mechanical property data and of the use of these materials at various shipyards led to the recommendation that certain laboratory investigations be conducted. This report describes the results of both small-scale and large-scale tests conducted on high-strength, low-alloy plate and weldments. These tests demonstrated that 8-in.-long flaws can initiate fast fracture at stresses below the yield strength of the material, that structural fracture resistance is increased by stiffeners, and that weldments can have fracture resistance equal to that of the base plate.

DD FORM 1 NOV 65 1473 (PAGE 1)

S/N 0101-807-6801

UNCLASSIFIED

Security Classification

SSC-232

Final Report

on

Project SR-177, "High-Strength, Low-Alloy Steel Weldments"

to the

Ship Structure Committee

STUDY OF THE FACTORS WHICH AFFECT THE ADEQUACY OF HIGH-STRENGTH, LOW-ALLOY STEEL WELDMENTS FOR CARGO SHIP HULLS

by

E. B. Norris, A. G. Pickett, and R. D. Wylie
Southwest Research Institute

under

Department of the Navy
Naval Ship Engineering Center
Contract No. N00024-67-C-5416

This document has been approved for public release and sale; its distribution is unlimited.

U. S. Coast Guard Headquarters
Washington, D. C.
1972

CONTENTS

SHIP STRUCTURE COMMITTEE

The SHIP STRUCTURE COMMITTEE is constituted to prosecute a research program to improve the hull structures of ships by an extension of knowledge pertaining to design, materials and methods of fabrication.

RADM W. F. Rea, III, USCG, Chairman
Chief, Office of Merchant Marine Safety
U. S. Coast Guard Headquarters

Capt. J. E. Rasmussen, USN
Head, Ship Systems Engineering
and Design Department
Naval Ship Engineering Center
Naval Ship Systems Command

Mr. K. Morland, Vice President
American Bureau of Shipping

Mr. E. S. Dillon
Chief
Office of Ship Construction
Maritime Administration

Capt. L. L. Jackson, USN
Maintenance and Repair Officer
Military Sealift Command

SHIP STRUCTURE SUBCOMMITTEE

The SHIP STRUCTURE SUBCOMMITTEE acts for the Ship Structure Committee on technical matters by providing technical coordination for the determination of goals and objectives of the program, and by evaluating and interpreting the results in terms of ship structural design, construction and operation.

NAVAL SHIP ENGINEERING CENTER

Mr. P. M. Palermo - Chairman
Mr. J. B. O'Brien - Contract Administrator
Mr. G. Sorkin - Member
Mr. H. S. Sayre - Alternate
Mr. I. Fioriti - Alternate

U. S. COAST GUARD

LCDR C. S. Loosmore, USCG - Secretary
CAPT C. R. Thompson, USCG - Member
CDR J. W. Kime, USCG - Alternate
CDR J. L. Coburn, USCG - Alternate

MARITIME ADMINISTRATION

Mr. R. Dashnaw - Member
Mr. A. Maillar - Member
Mr. R. Falls - Alternate
Mr. R. F. Coombs - Alternate

MILITARY SEALIFT COMMAND

Mr. R. R. Askren - Member
LTJG E. T. Powers, USNR - Member

AMERICAN BUREAU OF SHIPPING

Mr. S. G. Stiansen - Member
Mr. F. J. Crum - Member

OFFICE OF NAVAL RESEARCH

Mr. J. M. Crowley - Member
Dr. W. G. Rauch - Alternate

NAVAL SHIP RESEARCH & DEVELOPMENT CENTER

Mr. A. B. Stavovy - Alternate

NATIONAL ACADEMY OF SCIENCES - Ship Research Committee

Mr. R. W. Rumke, Liaison
Prof. R. A. Yagle, Liaison

SOCIETY OF NAVAL ARCHITECTS & MARINE ENGINEERS

Mr. T. M. Buermann Liaison

BRITISH NAVY STAFF

Dr. V. Flint, Liaison
CDR P. H. H. Ablett, RCNC, Liaison

WELDING RESEARCH COUNCIL

Mr. K. H. Koopman, Liaison
Mr. C. Larson, Liaison

I. INTRODUCTION

The use of high-strength, low-alloy quenched and tempered (HSLA-Q&T) steels of 100,000-psi minimum yield strength as materials of construction for merchant ship hull structures is the most recent application of this class of materials. The HSLA-Q&T steels have transition temperatures lower than merchant ship hull service temperatures, which obviates familiar brittle fracture, but have been found to be subject to unstable crack propagation at nominal stresses well below the strength capability of the material at temperatures in the ductile region.

The purpose of this report is to compare the structural behavior of ship structures built of HSLA-Q&T steel with those of similar structures made of carbon steel. This includes the measurement of notch toughness with practical specimens and the use of test results in estimating fracture safety. The relationships between specimen test results and hardware behavior, in lieu of service experience, must be evolved by correlation with structural prototype tests.

There are several candidate specimen test procedures and methods of data interpretation proposed by various investigators which may be useful in fracture analysis. Consequently, a study of the fracture behavior of HSLA-Q&T parent metal and weldments was undertaken. This program included tests on specimens ranging from large-scale structural models to small-scale laboratory tests following a survey of shipyard practice.

The survey was conducted on Phase I of the project and has been reported previously.[1] The premises obtained from Phase I to undertake Phases II and III are:

(1) Fast fracture is possible in HSLA-Q&T materials at nominal stresses less than the yield stress, the fracture stress being a function of the flaw size.

(2) Fast fracture of many of the HSLA-Q&T materials should be predictable by the fracture mechanics approach, but there is a general lack of quantitative data for accomplishing this.

The large-scale and small-scale test results, the subject of this report, were conducted under Phase II and III, respectively.

II. TEST PROGRAM

A. Scope

In Phase II, center-notched, wide-plate tension tests were performed to provide information for evaluating the effect of the following variables on the fast fracture behavior:

(1) *Heat input in the submerged arc (sub-arc) welding process.* Three heat input procedures were used. 65,000 J/in., 30,000 J/in. (used in ship construction at the present time), and a more economical 120,000 J/inch.

(2) *Temperature.* The emphasis was placed on temperatures considered representative of the minimum for ship structure service. Since the 1-1/4-in. plate being used in this program has a Nil Ductility Transition Temperature (NDTT) of -30° to 50°F, the 30°F test temperature is near the Fracture Transition Elastic (FTE) temperature for the base plate. A few tests were conducted at -50°F, near the NDTT of the base plate.

(3) *Flaw size and location.* Nominal 8- and 13-in. flaw lengths were evaluated. Flaws were placed in the heat-affected zone (HAZ) so that the fracture paths could seek the zone of least resistance, e.g., the parent metal, HAZ, fusion line, or weld metal.

(4) *Specimen width.* The performance of 30- and 120-in.-wide specimens were compared.

(5) *Structural reinforcements.* The 120 in.-wide plate specimen and one of the 30-in. specimens were prepared with tee stiffeners arranged and attached in a manner employed in container ships.

In Phase III, slow-bend fracture mechanics tests and notched impact tests were conducted to determine if they could be used to provide a correlation with the results obtained in Phase II. The following additional variables were studied:

(6) *Crack acuity.* Saw-cut, stress-corrosion, and fatigue cracks were compared.

(7) *Specimen thickness.* Notched impact fracture energy curves were developed on full thickness material to compare to Charpy V-notch data.

B. Test Materials

One ingot of A517D composition (heat no. 46538) was converted into 1-1/4- and 2-in.-thick plate especially for this program to eliminate the chemistry variable. This ingot was rolled into four plates as follows:

(1) Two plates were rolled to 1-1/4 in., the maximum permitted for Grade D, using 1.0 rolling ratio for enhanced transverse toughness.

(2) One plate was straight rolled to 1-1/4-in. thickness, with minimum transverse toughness typical of ship plate meeting A514D.

(3) One plate was rolled to 2-in. thickness to provide an unusually lean chemistry for this thickness which is not typical of either A514 or A517 specifications.

A second heat of A517D (heat no. 51252), 1-1/4 in. in thickness, was used for weld qualification tests. Heat no. 51301. A517E, 1-1/2 in. in thickness, was used for attaching the wide-plate specimen to the test machine.

The Mill Test Reports for the three heats, given in Table I, show that they meet the chemical and physical property requirements of ASTM A514 and A517 Grade D. The degree of cross-rolling is tabulated along with the Charpy-V results. Charpy-V results obtained by SwRI on these materials are given in Appendix A.

Both sub-arc and manual metal arc processes were used to fabricate test welds. Armco W-25 copper-coated weld wire and Linde 7095 flux was used for the sub-arc welds. E11018 welding electrodes were used for the manual welds, including the root pass, even though E8018 class 3 welding electrodes have been used for this early in the application of 517/514 steels in ships.

C. Selection of Welding Procedures

As previously reported[1], Phase I of this program included a survey of the fabrication procedures being employed by the various shipyards to construct ship hulls containing HSLA-Q&T materials. The results of the survey indicated that the sub-arc welding process was limited to a maximum heat input of 65,000 J/in., where 25,000 to 30,000 J/in. was most commonly used for joining these materials in the thickness ranges. However, the tests were programmed for 65,000 J/inch. The basic welding parameters used for this process appear as Procedure No. 1 in Table II and a typical joint design is shown in Figure 1.

Table 1. Mill Test Report Data

Chemical Analysis

Heat No.	C	Mn	P	S	Si	Cr	Mo	Ni	Cu	Ti	B	V
51301 Plate	0.17	0.52	0.014	0.022	0.29	1.69	0.56	-	0.27	0.064	0.002	-
51252 Plate	0.17	0.60	0.010	0.023	0.30	0.96	0.18	-	0.24	0.063	0.002	-
46538 Plate	0.17	0.56	0.010	0.022	0.31	1.04	0.21	-	0.25	0.077	0.002	-
516150 Weld Wire	0.12	1.70	0.008	0.006	0.27	0.45	0.50	1.98	0.12	-	-	0.008

Tensile Properties

Heat No.	Plate No.	Rolling Ratio	ASTM Spec	Thickness (in.)	Yield (ksi)	Ultimate (ksi)	Elongation (%)	R.A. (%)
51301	34646	1.2	A517E	1-1/2	114.4	128.8	22.0	61.5
51252	33697	2.4	A517D	1-1/4	107.2	117.0	21.0	62.9
46538	77293	1.8	A517D Mod.	2	106.1	117.8	17.0	62.8
46538	76784	1.0	A517D	1-1/4	105.2	117.0	17.0	60.8
46538	76785	1.0	A517D	1-1/4	111.5	119.7	19.0	64.0
46538	76786	22.0	A514D	1-1/4	118.5	126.3	19.5	67.2

Charpy-V Test Results

Heat No.	Plate No.	Average Room Temperature Results			Average−50°F Results		
		Ft-Lb	% Shear	Lat. Exp.	Ft-Lb	% Shear	Lat. Exp.
51301	34646L	-	-	-	36	82	29
	T	-	-	-	25	-	-
51252	33697T	-	-	.	18	75	15
46538	77293L	41	63	32	19	13	15
	T	36	53	30	11	0	9
46538	76784L	63	100	54	34	50	26
	T	44	100	37	25	45	19
46538	76785L	-	-	-	-	-	-
	T	-	-		-	-	-
46538	76786L	69	100	53	48	65	35
	T	28	100	24	17	37	14

Heat Treatment

Heat No.	Plate No.	Austenitizing Temp (°F)	Austenitizing Time (min)	Quenching Medium	Tempering Temp (°F)	Tempering Time (min)	Cooling Medium
51301	34646	1650	150	Water	1200	120	Water
51252	33697	1650	175	Water	1180	105	Water
46538	77293	1700*	180	Water	1150	140	Air
46538	76784	1650	114	Water	1160	99	Air
46538	76785	1650	114	Water	1160	99	Air
46538	76786	1650	120	Water	1160	99	Air

*Austenitized and water quenched twice.

Table 2. Welding Procedures Evaluated[a]

Parameter	No. 1	No. 2	No. 3	No. 4	No. 5
Process	Sub-arc	Sub-arc	Sub-arc	Manual	Manual
Electrode Type	Armco W25	W25	W25	E-11018	E-11018
Electrode Dia, in.	1/8	1/8, 5/32	1/8, 5/32	1/8, 5/32	1/8, 5/32
Max. Heat Input, J/in.	65,000	30,000	120,000	30,000	50,000
Amperage	500	340	500	115 to 150	115 to 150
Voltage	30	28	32	25 to 26	25 to 26
Travel Speed, in./min	14	23	8	7	4
Preheat, °F	100	100	100	200	100
Max. Interpass Temp, °F	150	150	150	300	150

(a) Tests were conducted on Plate No. 33697 of heat no. 51252.

Two radically different heat inputs were used for Test Procedures 2 and 3 (30,000 J/in. and 95,000 to 120,000 J/in., respectively), to determine what effect the size of the heat-affected zone would have on the explosion bulge performance of the weldments. In addition, two manual metal arc welding procedures were evaluated. As in the sub-arc welds, the heat input was varied: Test Procedure No. 4 utilizing 30,000 J/in. and Test Procedure No. 5 employing 50,000 J/inch. The two manual procedure welds were made with the joint in the fixed vertical (3 G) position and required all welding passes to be deposited uphill.

All welding was performed in a manner which would closely simulate shipyard practice, including the fact that all welds were made out-of-doors. Figure 2 shows a typical welding sequence. It should be noted that a temper bead technique was used for all welds. After completion of the first side of the weld (including the temper beads), the back side of the joint was air arc gouged to sound metal. This area was then ground and inspected by the magnetic particle technique and the first back-side pass was deposited. The joint was not allowed to cool below the preheat temperature until at least one-third of the total thickness of the weld was deposited. After welding was completed, the joints were ground flush to the base metal and magnetic particle inspected for evidence of surface defects. Radiographic inspection was used to determine the integrity of the weldment.

The first weld fabricated (Procedure No. 1) developed delayed transverse cracks in the weld metal. Subsequent radiographic inspection disclosed additional subsurface cracks. These were attributed to a number of possible factors: (1) welding out-of-doors in damp, cool weather, (2) marginal level of preheat, and (3) possible moisture in flux. The preheat was increased and the flux was specially dried, but the cracking in the sub-arc welds was not completely eliminated when using this heat of material.

D. Evaluation of Weld Procedure

The five procedures were evaluated on 1-1/4-in.-thick plate from heat no. 51252 by conducting tensile, bend, Charpy-V, and explosion bulge tests.

The results of tensile and bend tests run on the five test welds are given in Table III. Except for one HAZ fracture from Procedure No. 5, all tensile test results were satisfactory. All welding procedures except No. 2 passed the bend test. The weld metal deposited by sub-arc procedures at 25,000 to 30,000 J/in. had low ductility.

The results of Charpy V-notch tests conducted on the weld metal deposited by sub-arc procedures are presented in Figure 3. The toughness of the weld metal improves as the heat input is increased from 30,000 to 120,000 J/inch. The C_v properties of the weld metal deposited by the manual procedures, Figure 4, are better than those of the sub-arc-deposited weld metals, but show a reversed effect of heat input on shelf energy. The Charpy V-notch data are tabulated in Appendix A.

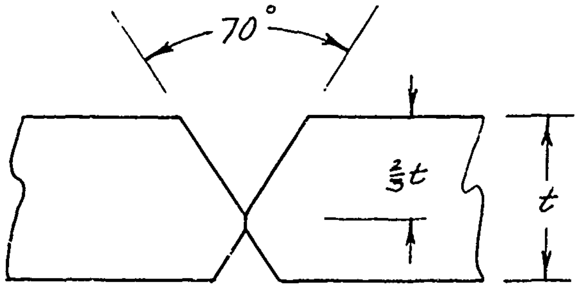

Fig. 1. Typical Weld Joint Design

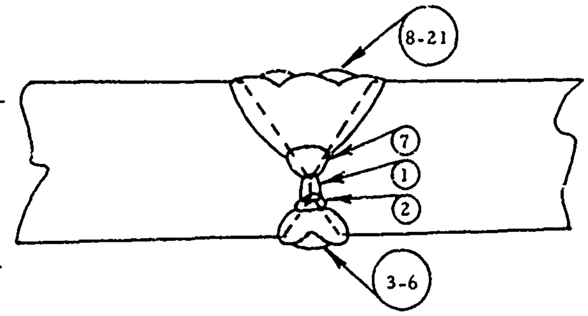

Fig. 2. Typical Welding Sequence

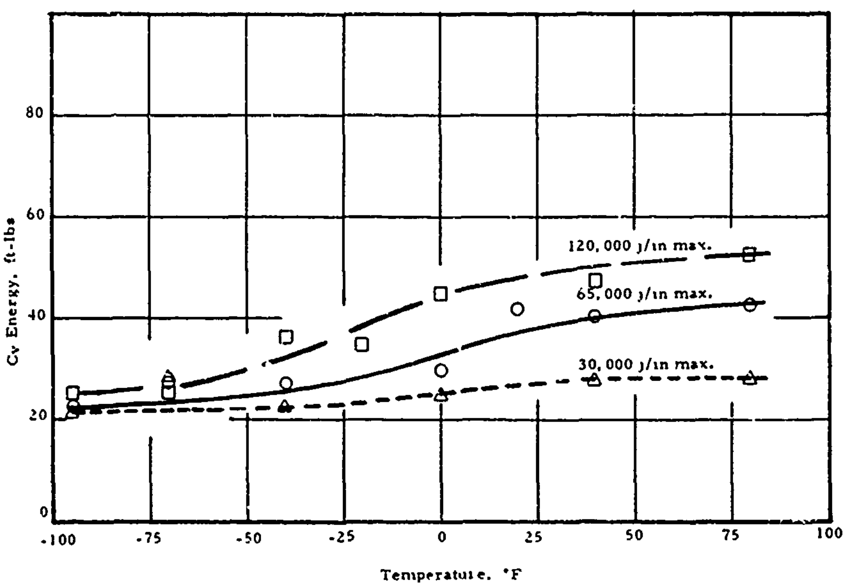

Fig. 3. C_v Energy Data on Sub-Arc Deposited Weld Metal

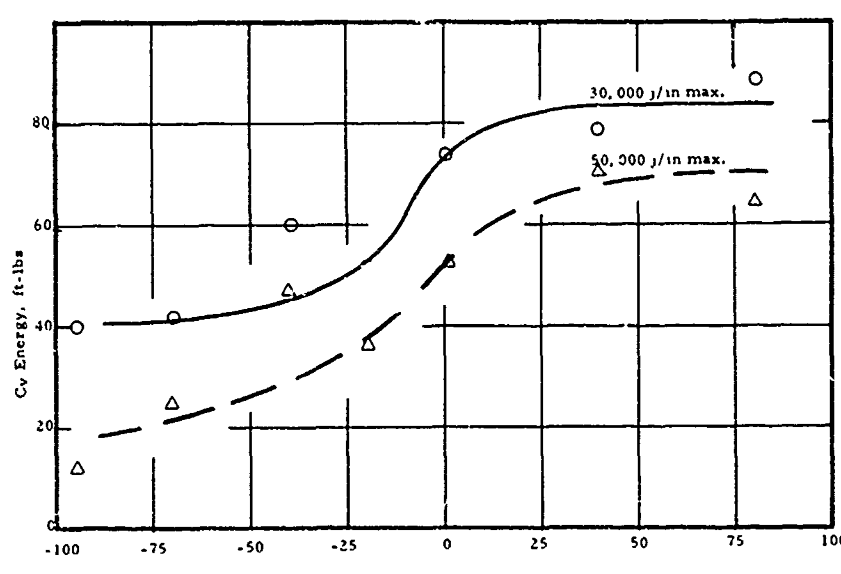

Fig. 4. C_v Energy Data on Manual Metal Arc Deposited Weld Metal

The C_v transition curve for the HAZ of the 65-kJ/in. weldment is compared to those obtained for the HAZ of the 30- and 120-kJ/in. weldments in Figure 5. The best performance was observed in the HAZ of the lowest heat input welds. The data are tabulated in Appendix A.

Explosion bulge crack starter specimens were fabricated with the primary rolling direction perpendicular to the weld. The weld reinforcement was removed by grinding. The tests were conducted at 0° and 30°F using a 12-lb charge and a 19-in. standoff. Test data, including photographs of the plates, are given in Appendix A. A brief description of the results of the explosion bulge tests follows.

Table 3. Transverse Tensile and Bend Test Results on Five Welding Procedures Studied

Welding Procedure[a]	Tensile Test Results			Side-Bend Test Results[b]
	Ultimate Tensile Strength (ksi)	Elongation (%)	Fracture Location	
SAW-65 kJ	121.0 120.9	20.2 22.4	Parent Parent	Passed[c]
SAW-30 kJ	111.3 112.4	24.2 23.0	Parent Parent	Failed[d]
SAW-120 kJ	118.2 119 6	22.1 21.0	Parent Parent	Passed
SMAW-30 kJ	116.5 116.4	22.1 21.9	Parent Parent	Passed
SMAW-50 kJ	117.0 117 5	16.8 20.6	HAZ Parent	Passed

(a) See Table II Plate material was 1-1/4-in. A517D, heat no. 51252.
(b) Per Section 26 of Rules for Building and Classing Steel Vessels, 1968.
(c) One of the four side-bend specimens showed a 3/16-in. opening after test. The defect was at the intersection of two weld beads and was representative of entrapped slag.
(d) Three of the four side-bend specimens failed in the weld metal by fracture at approximately a 90-deg bend angle. The fourth specimen showed three 3/4-in. lamination-type openings in the base metal at a 180-deg bend angle.

1. **SAW-65 kJ**

a. *30°F test.* This specimen was taken from the test weld plate so that a transverse welding crack was located at the center of the plate. The brittle weld crack starter bead was omitted. Cracking propagated into base metal, but did not follow weld metal or HAZ. Two cracks reached the elastic holddown area.

b. *0°F test.* Cracking occurred quite similar to that of the 30°F test.

2. **SAW-30 kJ**

a. *30°F test.* One crack propagated into base metal, but arrested very quickly (within 1 in. of weld). A second crack propagated about 4 in. along fusion line of weld.

b. *0°F test.* The tested plate is almost identical in appearance to the 30°F test plate.

3. **SAW-120 kJ**

a. *30°F test.* One crack propagated approximately 4 in. into base metal. Two fusion line cracks, each approximately 4 to 5 in. long, were also produced.

b. *0°F test.* Cracks extended to holddown region in both parent metal and fusion line.

4. **SMAW-30 kJ**

a. *30°F test.* Cracks were arrested in weld metal.

b. *0°F test.* Numerous cracks extended into parent metal and one reached the elastic holddown region.

5. **SMAW-50 kJ**

a. *30°F test.* Cracks were arrested in weld metal.

b. *0°F test.* Cracks were arrested in weld metal.

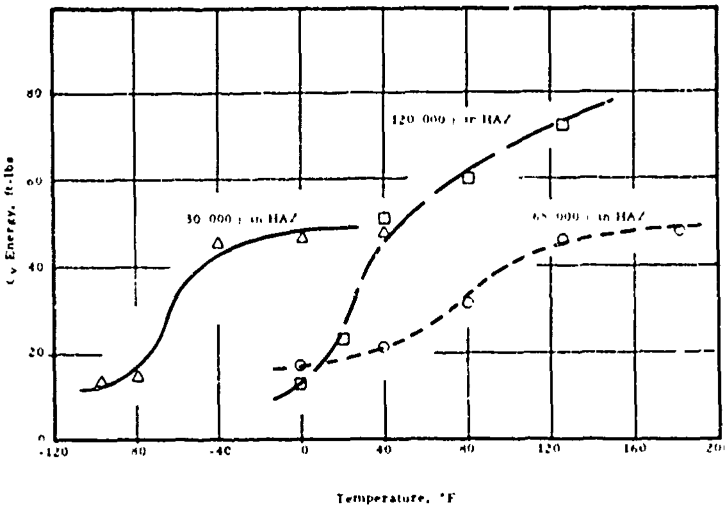

Fig. 5. Effect of Heat Input on Impact Properties of the HAZ of 1-¼" A517D Submerged Arc Weldments

The results of the explosion bulge crack starter tests conducted at 0° and 30°F to evaluate the five welding procedures indicate that weld metal deposited by the manual procedures has a greater ability to arrest a dynamic crack front than does the weld metal deposited by any of the sub-arc procedures. At 30°F, cracks were arrested in the weld metal deposited by either manual procedure. None of the sub-arc weld metals had sufficient toughness to arrest cracks. These results are consistent with the weld metal C_v data discussed earlier. The low heat input sub-arc weldment (SAW-30 kJ) performed best. However, the more economical intermediate heat input weldment (SAW-65 kJ) also produced satisfactory welds, since the only cracks which propagated to the elastic holddown region were located in parent metal. The high heat input weldment (SAW-120 kJ) exhibited the greatest amount of cracking in the weld fusion line or HAZ, reaching the elastic holddown region when tested at 0°F. These results are in general agreement with information obtained in the Phase I survey, since some shipyards had reported that they were unable to qualify a sub-arc procedure for the A517D alloy in 1-in. thickness unless the heat input was kept considerably under 65,000 J/inch.

E. Phase II Large-Scale Specimen Tests

Two sizes of large-scale specimens, 30 and 120-in. wide, were selected for use in this phase of the program. The majority of specimens were prepared with a 65-kJ/in. weldment in the test section. One specimen was prepared with a 120-kJ/in. weldment and one specimen had no weld in the test section.

Ten 30-in.-wide fracture toughness specimens and one 120-in.-wide simulated structure specimen, all containing a central notch through the plate, were fabricated and tested. The basic 30-in.-wide specimen (notch omitted) is shown in Figure 6. One 30-in.-wide specimen was fabricated with tee stiffeners on one surface to simulate the strength of deck of a cargo ship, as shown in Figure 7.

Nine of the 30-in.-wide specimens (including the specimen with tee stiffeners) contained a central through-the-thickness flaw shown as configuration "A" in Figure 8(a). The tips of the flaws were located in parent metal, weld metal, or the HAZ, also as illustrated in Figure 8(a). One 30-in.-wide specimen was notched in the HAZ with flaw configuration "B" as shown in Figure 8(b).

The 120-in.-wide specimen was fabricated with a flaw having configuration "A" in the HAZ of the test weld. The fabrication sequence utilized in the construction of this specimen is shown in Figure 9. This specimen was also reinforced with tee stiffeners, the locations of which are shown in Figure 10.

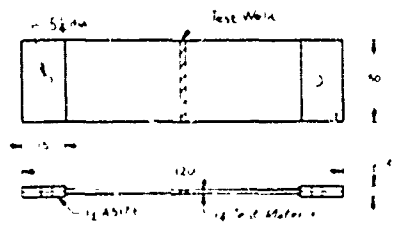

Fig. 6. Basic 30-Inch Wide Test Specimen

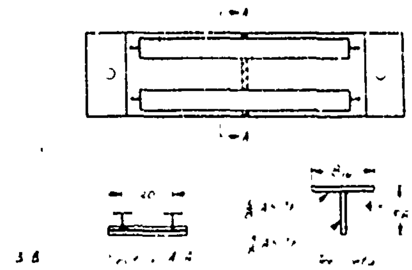

Fig. 7. Tee-Stiffened 30-Inch Wide Test Specimen

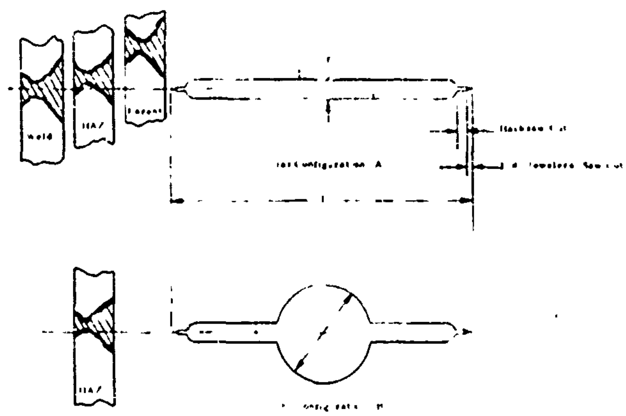

Fig. 8. Through-Wall Flaw Configurations

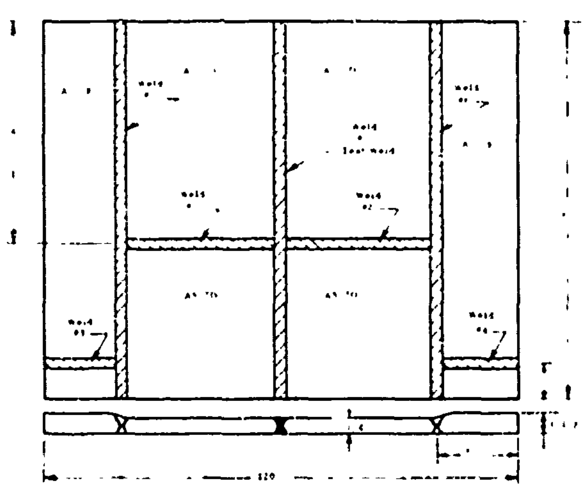

Fig. 9. Fabrication Sequence for 120-Inch Test Specimen

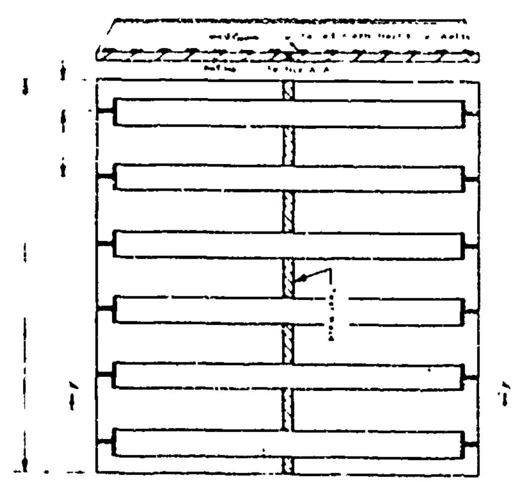

Fig. 10. Location of Tee-Stiffeners on 120-Inch Specimen

(See Fig. 7 for Detail of Tee)

No cracking was experienced in welding this heat of 1-1/4-in.-thick A517D to itself. However, during the fabrication of the wide-plate specimen, it was necessary to join sections of 1-1/2-in.-thick A517E material to the 1-1/4-in. A517D test plate at each end. After the first weld joint had been completed, it was visually and magnetic particle inspected. Numerous transverse cracks were noted in this weld. This joint was cut out and rewelded.

Another such problem was encountered during testing of the first 30-in. specimen. The test was discontinued when the specimen failed at the grip-to-plate joint, again joining 1-1/4-in.-thick A517D to the 1-1/2-in. A517E grip material. These joints were rewelded after modification of the grip joint geometry and an adjustment of the welding procedure which involved a buttering operation on the grip.

Each test weld was inspected as follows

(1) Visual inspection of each weld bead

(2) Magnetic particle inspection of the back-side grindout

(3) Magnetic particle and visual inspection of the completed and ground joint

(4) Radiographic examination of the entire length of each test weld.

All defects found in excess of the requirements of the ASME Section VIII Boiler and Pressure Vessel Code were removed and rewelded in accordance with the original welding procedure

The tee stiffeners were fabricated from A517F plate (3/8- and 5/8-in. thickness). The tee was formed by fillet welding the sections together using the manual metal arc process and E-11018 electrodes. The tee's were then joined to the test specimen with a chained intermittent fillet weld in a manner typical of that employed in ship hull construction, as was detailed in Figure 7.

The through-thickness flaws in the wide-plate specimens were prepared by generating a stress-corrosion crack from a mechanical notch. Initially, the notch root was cold-pressed with a knife edge, as shown in Figure 11(a), but it was difficult to generate a stress-corrosion crack. A modified notching procedure, illustrated in Figure 11(b), proved successful.

An ultrasonic monitoring system was set up to follow the growth of stress-corrosion cracks and slow crack extension, if any, during the conduct of the 120-in.-wide plate fracture toughness test. The basic setup used a send-and-receive technique, with three pairs of transducers positioned beyond the crack tip. The system was used through the completion of the 120-in.-wide plate test. After that time, experience had indicated that no significant slow growth occurred on loading prior to fast fracture and stress-corrosion crack extension could be followed adequately by visual observation. Therefore, the use of this technique was discontinued.

The plates were cooled to the test temperature with dry ice which did not contact but was held close to both plate surfaces by wire screening. Temperatures were measured with thermocouples which had been soldered to the specimen on both surfaces and on both sides of the central flaw, but slightly offset from the expected line of fracture propagation. The tensile loads were applied with a 15,000,000-lb hydraulic machine designed and built by SwRI for an earlier brittle fracture program.[2]

The applied loads were determined from electrical resistance strain gages attached to both surfaces of each specimen at a point midway between the flaw and one end of the specimen. Strain gages were also applied to the weld metal and HAZ in the test section area so that the nominal net section stress could be checked. In most cases, longitudinal gages were employed, but two-gage rosettes were also utilized.

F. Phase III Small-Scale Specimen Tests

Two types of small-scale specimen tests were evaluated in this phase of the program. Slow-bend tests were performed on notched fracture mechanics-type specimens to determine if a correlation could be established with the results obtained on wide-plate tests. Notched impact tests were run on the base materials to try to establish a transition temperature for the upper bound of dynamic plane strain notch toughness behavior for the 1-1/4- and 2-in. thicknesses.

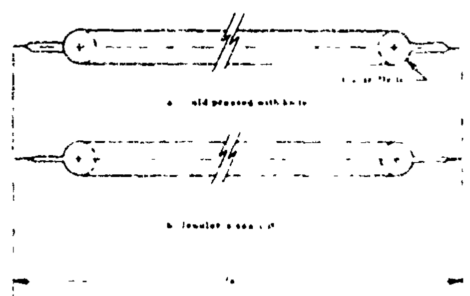

Fig. 11. Plan View of Flaw Showing Details of Two Methods Used to Sharpen the Tips

1. Slow-Bend Tests

All but one of the slow-bend tests were run on specimens fabricated as shown in Figure 12. The remaining slow-bend specimen was prepared with a Chevron notch as described in Figures 4 and 6 of ASTM Method E399, "Tentative Method of Test for Plane-Strain Fracture Toughness of Metallic Materials."

Other variables introduced into the small-scale specimen test program were notch acuity (jeweler's saw-cut, stress-corrosion, and fatigue-generated cracks), notch location (parent metal and heat-affected zone), side grooving, and welding heat input. Notch acuity was investigated to assist in analyzing the data from wide-plate tests which had been performed on specimens having stress-corrosion cracks generated from the tip of a jeweler's saw cut.

The slow-bend specimens were loaded in three-point bending while recording the crack opening displacement as a function of applied load to fracture. The critical value of K, K_Q, was calculated by the secant method described in ASTM E399.

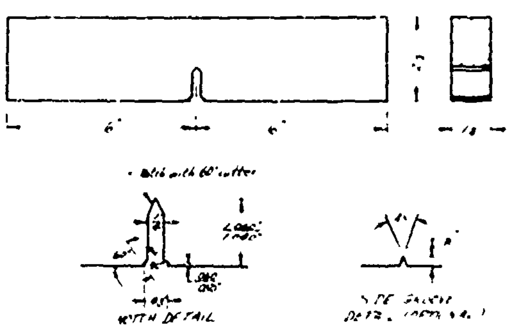

Fig. 12. Slow Bend Fracture Toughness Specimen

2. Notched Impact Tests

Notched impact tests were performed on base metal only using the specimen shown in Figure 13. The specimens representing 2-in. plate material were machined down to 1-1/4-in. thickness to eliminate the geometry effect and to develop only the metallurgical effect on notch impact toughness.

Fracture energy as a function of test temperature was determined by breaking the specimens in a 5000-ft-lb capacity dynamic tear-test machine after conditioning the specimens for an hour in a liquid bath held at the desired test temperature.

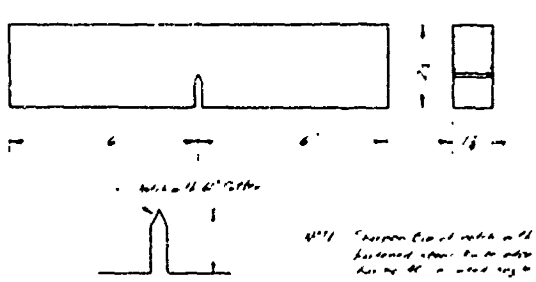

Fig. 13. Notched Impact Test Specimen

III. RESULTS OF CENTER-NOTCHED, WIDE-PLATE TESTS

Fifteen tests were run on eleven center-notched specimens, at a temperature of 32°, 0°, or 50°F, applying a tensile load perpendicular to the test weld and the flaw. The strain gage data obtained on these are contained in Appendix C.

In addition to obtaining data for calculating the critical stress intensity factors for the initiation of fast fractures, macrosections through selected fractures were examined so that the location of the fracture path relative to the weldment microstructure could be determined. The fractures veered into the base metal more often than staying in the fusion line or HAZ. None of the fractures propagated through weld metal.

The results of the tests conducted at a test temperature of 32°F are summarized in Table IV, and those conducted at lower temperatures are given in Table V. The stress intensity factors were calculated as K_{max} for those cases in which the specimen did not fail. K_c was calculated whenever a distinct pop-in or complete fracture occurred. Since the plate thickness is not adequate to guarantee a valid K_{Ic} for this material, an estimated value for K_{Ic} (called K_T) was calculated from the relationship

$$K_T = \frac{K_c}{(1 + 1.4\beta_Q)^{1/2}}$$

where

$\beta_Q = \frac{1}{t}\left(\frac{K_c}{\sigma_{ys}}\right)^2$; t is the plate thickness in inches, and σ_{ys} is the yield strength of the material in psi.

The fracture of Specimen No. 1 occurred primarily in the fusion line. Specimen No. 2, however, failed in the fusion line from one end of the flaw, but fractured in the base metal from the other end, Figure 14. The fracture appearances of Specimens Nos. 3 and 5 were strikingly similar to Specimen No. 2, each fracturing along the fusion line from one end of the flaw and primarily in parent metal from the other end. Specimen No. 4 was not taken to complete fracture. The wide-plate specimen also fractured in the parent metal at one end and in the fusion line at the other. Sections taken within the region of pop-in are presented in Figure 15 showing that fracture initiation occurred along the fusion line. The arrest of the initial pop-in fracture occurred after the path had shifted to the base metal (Fig. 16). The stress-corrosion crack at one end of the central flaw was found to lie primarily in the HAZ (Fig. 17).

Specimen No. 6 fractured through parent metal from both ends of the flaw. Specimen No. 7 was an all-parent metal specimen. Specimens Nos. 8 and 9 failed in the fusion line from one end of the flaw and in parent metal from the other end of the flaw. The fracture in Specimen No. 10 propagated essentially all the way in parent material, although the fracture curved back to the fusion line near each edge of the specimen.

Table 4. Summary of Center-Notched Wide-Plate Test Results at 32°F

Test No.	Specimen No	Description[a]	Run No.	Initial Flaw Size[a] (in.)	Result	Average Stress (ksi) Gross	Average Stress (ksi) Net	Fracture Location[c]	K_c[c] (ksi$\sqrt{in.}$)	K_T[c] (ksi$\sqrt{in.}$)
1	2	30 in.–side grooved	3	13.2	Fast fracture	28.9	64.0	F, B	168	114 est[f]
2	1	30 in.–partially side grooved	2	12.6	Fast fracture	37.0	64.0	F	188	122 est
3	3	30 in.–side grooved	1	8.8	Pop-in	27.3	48.0	F	119	-
4	3	30 in.–side grooved	2	11.2	Fast fracture	29.1	58.0	F, B	134	102 est
5	WP-1	120 in.–not grooved with beams	1	8.8	Out of stroke	52.0[d]	57.0[d]	-	(194)[g]	
6	WP-2	120 in.–not grooved, beams cut	1[e]	8.8	Pop-in	41.0	44.0	F	153	101 est
7	WP-2	120 in.–not grooved, beams cut	2	24.0	Fast fracture	55.0	69.0	F, B	343	157 est
8	4	30 in.–not grooved	2	8.0	Pop-in	45.1	61.0	-	172	114 est
9	5-1	30 in.–not grooved, with beams	1	8.3	Out of stroke	62.4[d]	86.0[d]	-	(237)[g]	
10	5-2	30 in.–not grooved, beams cut	2	8.3	Fast fracture	53.7	74.0	F, B	204	130 est

(a) All flaws in HAZ of 65-kJ sub-arc weld.
(b) F = fusion line, B = base metal.
(c) Uncorrected for plastic zone size.
(d) Includes cross-sectional area of beams.
(e) New flaw.
(f) Equations of Section III.
(g) Value of K at maximum load–specimen did not fail.
Based on plate formula–ignoring stiffener geometric effect.

Table 5. Summary of Center-Notched Wide-Plate Test Results at 0° and -50°F

Test No.	Specimen No.	Description[a]	Test Temp	Run No.	Initial Flaw Size (in.)	Result	Average Stress (ksi) Gross	Average Stress (ksi) Net	Fracture Location[b]	K_c[c] (ksi$\sqrt{in.}$)	K_T[c] (ksi$\sqrt{in.}$)
11	6	65-kJ HAZ	0°F	1	8.5	Fast fracture	44.9	61.3	B	171	115 est[d]
12	7	Parent	-50°F	1	8.5	Fast fracture	34.5	47.0	B	131	101 est
13	8	65-kJ Weld	0°F	1	8.5	Fast fracture	43.5	59.3	F, B	166	113 est
14	9	120-kJ HAZ	0°F	1	8.5	Fast fracture	31.2	42.5	F, B	119	94 est
15	10	65-kJ HAZ	-50°F	1	8.5	Fast fracture	30.4	41.4	F, B	116	92 est

(a) All tests were conducted on 30-in. specimens that had not been side grooved. Flaw located as indicated.
(b) F = fusion line, B = base metal.
(c) Uncorrected for plastic zone size.
(d) Equations of Section III.

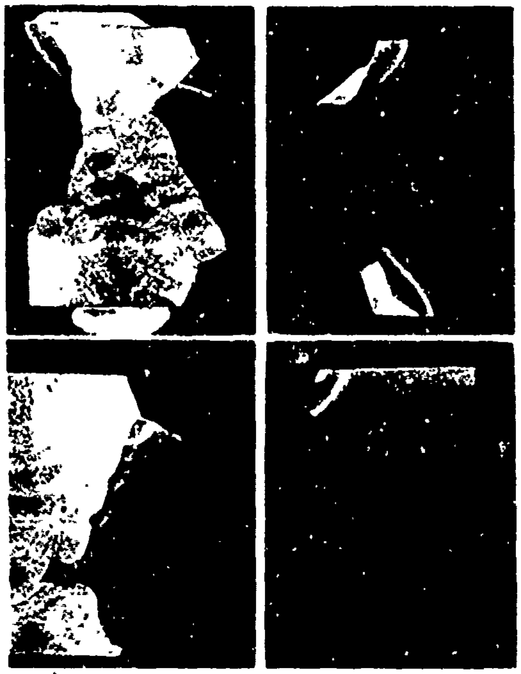

Fig. 14. Cross-Section Showing Fracture Paths in Specimen Number Two (30 Inch Wide)

Fig. 15. Cross-Section Through Pop-In Fracture in 120-Inch Specimen

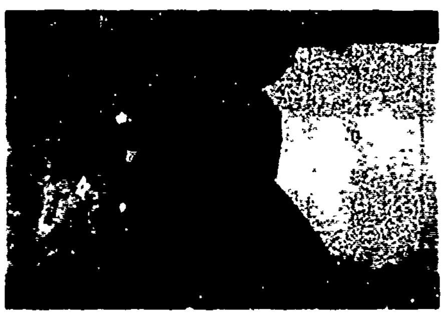

Fig. 16. Cross-Section Through the Pop-In Arrest Zone in the 120-Inch Specimen

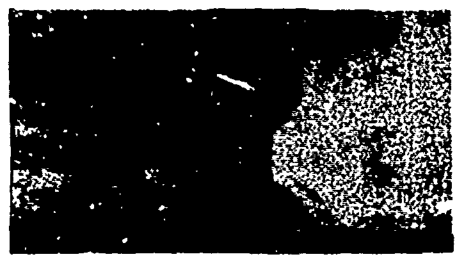

Fig. 17. Cross-Section Through the Stress Corrosion Crack at One End of Flaw in the 120-Inch Specimen

IV. RESULTS OF SMALL-SCALE SPECIMEN TESTS

A. Static Test Results

Seventeen slow-bend (notched bar in three-point loading) 1-1/4-in.-thick specimens were tested at temperatures of 32°, 0°, and -50°F. All specimens were oriented transverse to the primary rolling direction. In addition to temperature, the variables were:

(1) Type of notch:

- Stress corrosion
- Fatigue crack
- Jeweler's saw cut.

(2) With and without side groove.

(3) Material.

- 1-1/4-in. base plate
- 2-in. base plate.

(4) Welding procedure with notch in HAZ:

- 30-kJ heat input
- 65-kJ heat input
- 120-kJ heat input.

Table 6. Static (Slow-Bend) Specimen Fracture Toughness Test Results on A517D Plate (Heat No. 46538)

Specimen No	Material	Notch Preparation and Depth	Side Grooved	Test Temp (°F)	Fracture Appearance (% Shear)	K_Q (psi$\sqrt{in}$)
1-1/4B-7	1-1/4-in. base plate	S.C. (1.398 in.)	No	0	50	118,000
1-1/4B-8		S.C. (1.492 in.)	No	50	30	138,000
1-1/4B-9		S.C. (1.198 in.)	Yes	0	5	130,700
1-1/4B-10		Fatigue per ASTM (1[illegible].37 in.)	No	-50	30	93,200
2B-7	2-in. base plate	S.C. (1.399 in.)	No	0	25	129,800
2B-8		S.C. (1.229 in.)	No	-50	10	104,900
2B-9		S.C. (1.322 in.)	Yes	0	5	136,800
HZ65-1	65-kJ HAZ	S.C. (1.212 in.)	No	-50	5	114,500
HZ65-2		Fatigue (1.278 in.)	No	0	40	119,000
HZ65-3		S.C. (1.177 in.)	No	0	60	114,000
HZ65-4		Jeweler's saw cut (1.158 in.)	No	0	5	106,000
HZ65-5		S.C. (1.152 in.)	No	32	45	119,300
HZ65-6		S.C. (1.162 in.)	Yes	0	30	116,100
HZ65-7		Jeweler's saw cut (1.168 in.)	Yes	0	20	104,800
HZ65-8		Fatigue (1.224 in.)	Yes	0	10	116,900
HZ30-1	30-kJ HAZ	S.C. (1.184 in.)	No	0	55	119,000
HZ120-1	120-kJ HAZ	S.C. (1.214 in.)	No	0	30	102,900

The test results are summarized in Table VI, and the crack opening displacement versus load curves are shown in Appendix D.

The K_Q values demonstrate that, as expected, the specimen thickness was less than required for K_{Ic} measurement. The load-displacement records and fracture appearance indicate that the specimen tests results were in the fast fracture regime, i.e., pop-in was not succeeded by arrest. No effect of the variables studied is evident in the results. The data scatter is not excessive for material in the transition range, and examination of the fractures reveals that the scatter is at least in part attributable to the effect of metallurgical discontinuities such as laminations. The fracture appearance data in Table VI is reported as percent shear, including shear lips along any laminations.

The fracture surfaces of slow-bend specimens machined from 1 1/4-in. base plate are shown in Figure 18. Specimen No. 10 was fatigue precracked while the others were sharpened by stress-corrosion prior to testing. The presence of metallurgical discontinuities at the root of the precrack may have contributed to the higher value of K_Q. However, this phenomenon did not appear to have the same effect on Specimens Nos. 7 and 9 (left-hand side of Fig. 18). The fracture surfaces of specimens machined from 2-in. plate are shown in Figure 19. Again, the effect of discontinuities is not conclusive, but the shallower precrack on Specimen No. 9 may have affected the results.

No effect of notch acuity was evident from the results conducted on 65-kJ/in. HAZ specimens shown in Figure 20. Here again, the presence of a metallurgical discontinuity in Specimen No. 6 may have clouded the picture. There was little effect of metallurgical condition on K_Q as illustrated by the series shown in Figure 21. Figure 22 shows two series of specimens, the vertical representing the effect of test temperature and the horizontal representing the effect of notch acuity on K_Q of the HAZ of a 65-kJ/in. weldment.

The data trends with temperature and welding procedure are as expected but are less significant than data scatter so that the 50°F data [below nil ductility transition temperatures (NDTT)] encompass the higher temperature fracture toughness results.

B. Notched Impact Test Results

The impact test data are tabulated in Appendix F. The fracture energy transition curves are presented in Figures 23 and 24. As shown by these figures, the drop weight NDTT, determined per ASTM E208 with Type P-1 specimens, correlate with the beginning of the energy transition curve for these specimens. Also, the Charpy-V fracture appearance transition temperature (C_v FATT) is surprisingly close to the NDTT and underestimates considerably the full thickness impact fracture appearance transition temperature (1-1/4 FATT) which may be considered to be an approximation to the temperature at which significant energy is dissipated by shear to arrest propagating cracks. This is illustrated by the agreement between the 1-1/4 FATT and the 50-percent energy transition temperature (1-1/4 ETT) defined as the temperature at which fracture energy is equal to the average of the lower shelf and upper shelf fracture energies. These data indicate that the slow-bend specimens were tested in the transition temperature range for this thickness of material.

The fracture surfaces exhibited shear lips along metallurgical discontinuities as well as at the specimen edges. A corresponding increase in fracture energy was noted in such cases. For example, the 1-1/4-in. notched impact specimen tested at 40°F (see Fig. 23) appears to fall above the trend line for the rest of the data in this series. The fracture appearance data, given as percent shear, include these internal shear lips.

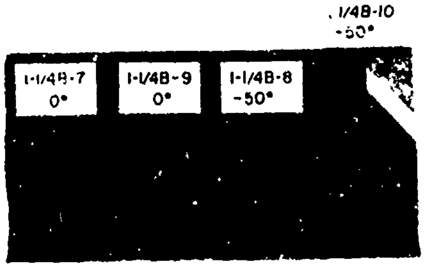

Fig. 18. Fracture Surfaces of 1-¼-Inch Base Plate Slow Bend Specimens

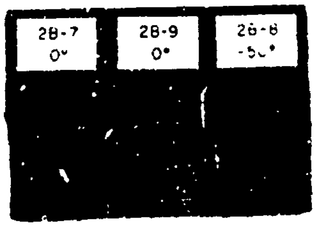

Fig. 19. Fracture Surfaces of 2-Inch Plate Slow Bend Specimens

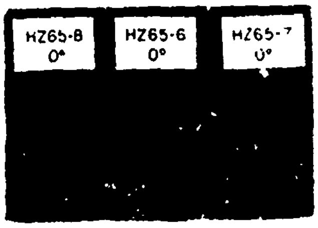

Fig. 20. Fracture Surfaces of 65 Kj Slow Bend Specimens With Three Notch Acuities

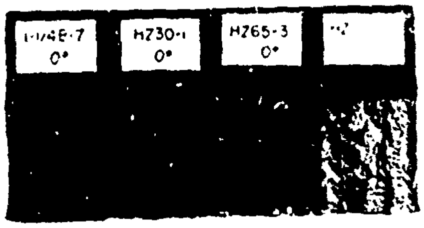

Fig. 21. Fracture Surfaces of Specimens Representing Base Material and Three Welding Heat Inputs

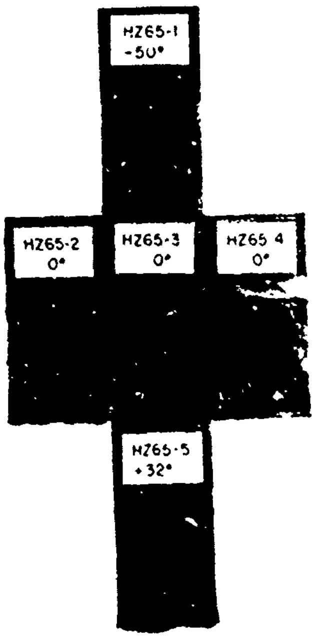

Fig. 22. Fracture Surfaces of 65 Kj Weldment Specimens.

Horizontal - Effect of Notch Acuity
Vertical - Effect of Temperature

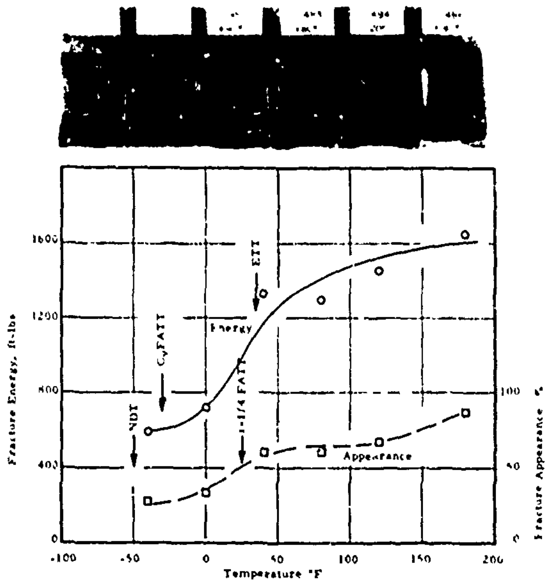

Fig. 23. Impact Test Results on 1-¼-Inch Base Plate

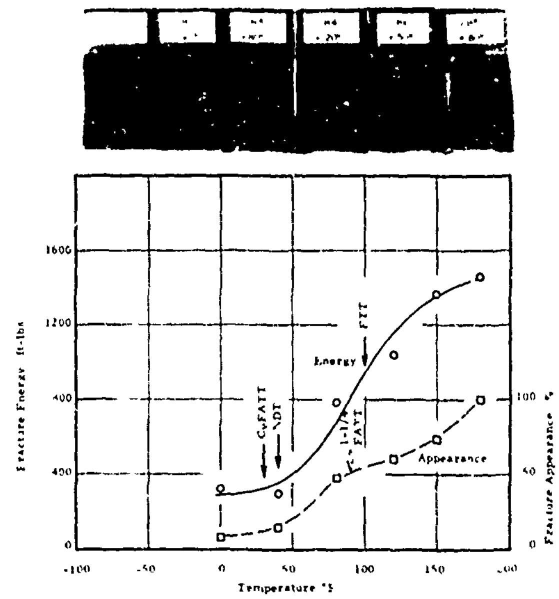

Fig. 24. Impact Test Results on 2-Inch Base Plate

V. SUMMARY

The test results are in accordance with the premises of Phase I[1] which were the basis for this test program. The data are also in agreement with the data obtained by previous programs and by others on other A514 and A517 materials.

The test results obtained in this program demonstrate that for the two heats of steel evaluated:

(1) Fast fracture of wide-plate specimens containing large flaws occurs at nominal (and net) stress levels less than yield strength up to 32°F.

(2) Some agreement is obtained between fracture toughness measured by wide-plate specimens and slow-bend specimens using fracture mechanics equations.

(3) Structural fracture resistance is increased by stiffeners as would be expected by fracture analysis models considering stiffener effects.[3,4,5]

(4) Full thickness impact test fracture appearance is a better index of transition behavior than Charpy-V test results for this material.

(5) Weldments made with heat inputs of 25 to 50 kJ/in. can have fracture resistance equal to that of the base plate.

Extensive testing of materials needs to be performed to provide a statistical design basis for use of HSLA-Q&T materials.

VI. REFERENCES

1. Lowenberg, A. L., Norris, E. B, Pickett, A. G., and Wylie, R. D., "Study of Factors Which Affect the Adequacy of High-Strength Low-Alloy Steel Weldments for Cargo Ship Hulls," *SSC-199*, AD 692262, August 1969

2. Sherman, R., "Simulated Performance Testing for Ship Structure Components," *SSC-204*, 1970.

3. Romauldi, J. P., "Fracture Arrest Design Considerations," Proceedings of the Crack Propagation Symposium, Cranfield, pp 287-302, September 1961.

4. Weiss, V., Grewal, K. S., and Sessler, J., "The Effect of Testing System Stiffness on Fracture," Air Force Materials Laboratory Technical Documentary Report No. ML-TDR-64-150.

5. Boyd, G. Murray, "Fracture Design Practices for Ship Structures," Fracture, Chapter 5, Edited by H. Liebowitz, Academic Press, 1969.

APPENDIX A

DATA ON TEST MATERIALS AND WELDMENTS

Table A-I. SwRI Charpy V-Notch Test Results, 2-In. ASTM A517D Modified, Firebox Quality Heat No. 46538, Plate 77293

Longitudinal[a]				Transverse[a]			
Temp (°F)	Energy (ft-lb)	% Shear	Lat. Exp.	Temp (°F)	Energy (ft-lb)	% Shear	Lat. Exp.
-85	9	3	[illegible]	-85	9	3	6
-60	16	8	10	-60	8	5	5
-20	22	15	13	-20	19	8	11
0	29	25	18	0	23	13	15
30	36	42	24	30	31	27	21
60	54	85	39	60	37	35	27
100	60	93	33	90	44	75	34

(a) Average of 3 tests at each temperature.

Table A-II. SwRI Charpy V-Notch Test Results 1-¼-In. ASTM A517D, Firebox Quality

Heat No. 46538, Plate 76784							
Longitudinal[a]				Transverse[a]			
Temp (°F)	Energy (ft-lb)	% Shear	Lat. Exp.	Temp (°F)	Energy (ft-lb)	% Shear	Lat. Exp.
-85	26	13	15	-85	18	11	9
-60	30	27	18	-60	22	18	13
-40	33	30	21	-40	-	-	-
-20	46	72	27	-20	30	40	20
0	55	90	33	0	31	43	20
30	64	100	44	30	41	83	25
60	68	100	38	60	48	100	35
90	-	-	-	90	47	100	34
Heat No. 46538, Plate 76785							
-90	20	10	11	-85	18	13	10
-60	2[illegible]	17	13	-60	16	12	9
-40	3[illegible]	25	18	-40	-	-	-
-20	34	50	21	-20	24	28	17
0	44	85	21	0	30	45	19
30	46	95	34	30	34	53	23
60	49	100	37	60	41	87	29
90	-	-	-	90	47	100	35
Heat No. 46538, Plate 76786							
-90	29	13	16	-90	11	9	7
-60	37	30	21	-60	15	18	9
-40	51	48	31	-40	-	-	-
-20	52	72	34	-20	20	22	13
0	62	85	43	0	22	25	15
30	77	97	47	30	25	35	19
60	81	100	51	60	29	98	22
100	-	-	-	100	32	100	21

(a) Average of 3 tests at each temperature.

Table A-III. Weld Metal Charpy V-Notch Test Results for Five Welding Procedures[a]

Temp (°F)	Absorbed Energy (ft-lb) for Each Welding Procedure[b]				
	No. 1	No. 2	No. 3	No. 4	No. 5
-95	22	32	25	40	12
-70	27	29	25	42	25
40	27	23	36	60	47
-20	--	-	35	52	37
0	30	25	45	74	53
20	42	-	-	-	-
40	40	28	47	78	72
80	43	28	53	88	64
120	--	42	-	-	.

(a) 1. Sub-arc with 65,000-J/in. max heat input
2. Sub-arc with 30,000-J/in. max heat input
3. Sub-arc with 120,000-J/in. max heat input
4. Manual Metal Arc with 30,000-J/in. max heat input
5. Manual Metal Arc with 30,000-J/in. max heat input.

(b) Average of three tests.

Table A-IV. HAZ Charpy V-Notch Test Results for Three Sub-Arc Procedures[a]

Temp (°F)	Absorbed Energy (ft-lb) for Each Welding Procedure[b]		
	No. 1	No 2	No. 3
-96	-	14	
-80		15	--
-40	-	46	
0	17	46	14
20		-	24
40	21	47	51
80	32		60
125	46		73
180	48		

(a) 1. Sub-arc with 65,000-J/in max heat input
2. Sub-arc with 30,000-J/in. max heat input
3. Sub-arc with 120,000-J/in. max heat input.

(b) Average of two tests.

Table A-V. Explosion Bulge Test, Thinning and Bulge Height Data

Plate No	Welding Procedure No.[a]	Test Temp (°F)	Max % Reduction		Profile Bulge Height	
			Base Plate	Weld Metal	Across Weld	Along Weld
1A	1	+30	1.9	1.5	2-11/16	2-11/16
1B	1	0	1.9	2.7	2-3/16	2-5/16
2A	2	+30	3.0	2.3	1-1/2	1-1/4
2B	2	0	2.2	2.3	1-5/8	1-3/4
3A	3	+30	2.3	1.5	2-1/16	2
3B	3	0	1.5	1.9	2-9/16	2-7/16
4A	4	+30	3.4	3.0	1-3/8	1-1/2
4B	4	0	3.0	3.0	1-1/2	1-5/8
5A	5	+30	2.6	2.3	1-3/8	1-3/8
5B	5	0	2 6	2.6	1-3/8	1-1/2

(a) 1 Sub-arc with 65,000-J/in. max heat input
2. Sub-arc with 30,000-J/in. max heat input
3. Sub-arc with 120,000-J/in max heat input
4. Manual Metal Arc with 30,000-J/in. max heat input
5. Manual Metal Arc with 30,000-J/in. max heat input.

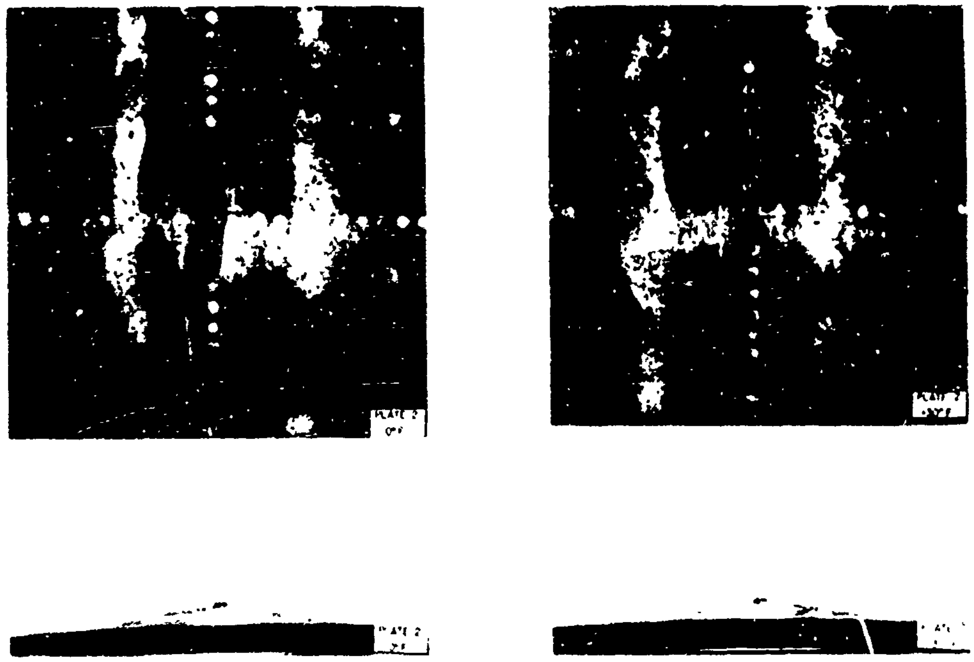

Fig. A-1. Explosion Bulge Plates from SAW-30Kj Weldment

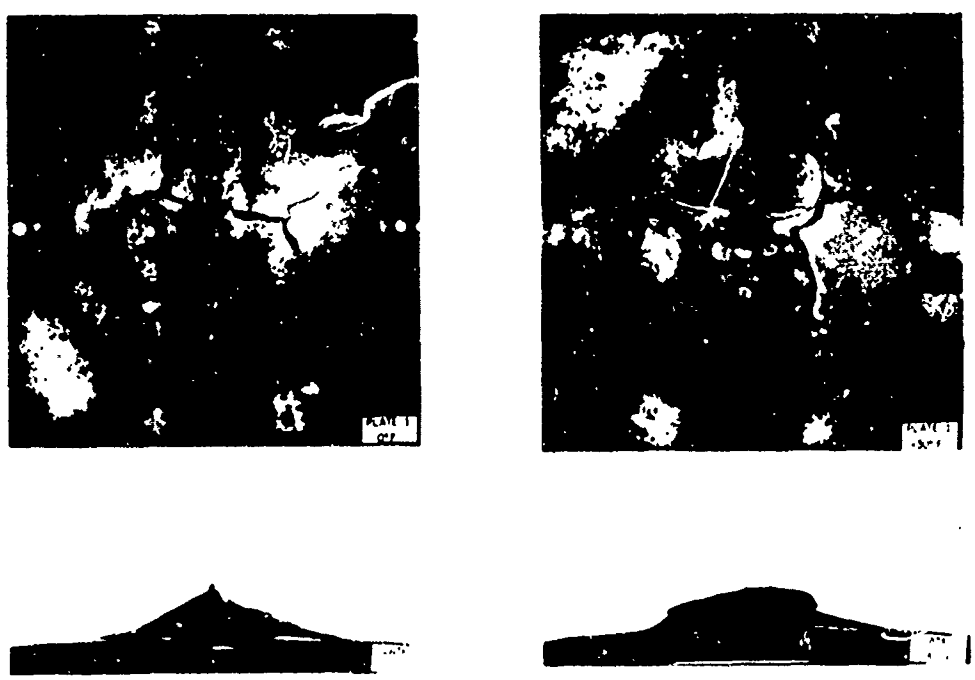

Fig. A-2. Explosion Bulge Plates from SAW-65Kj Weldment

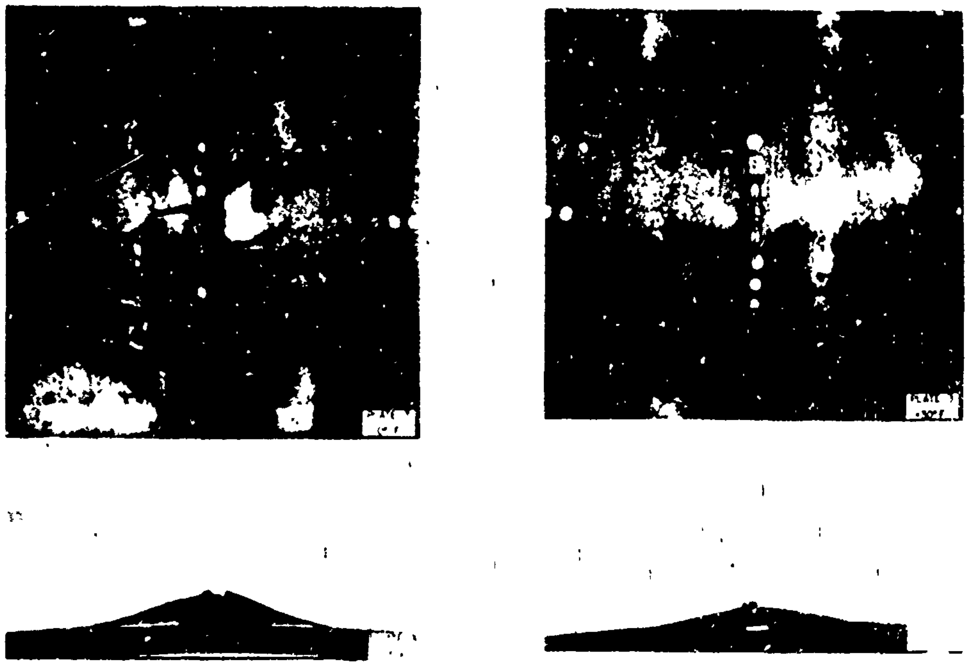

Fig. A-3. Explosion Bulge Plates from SAW-120Kj Weldment

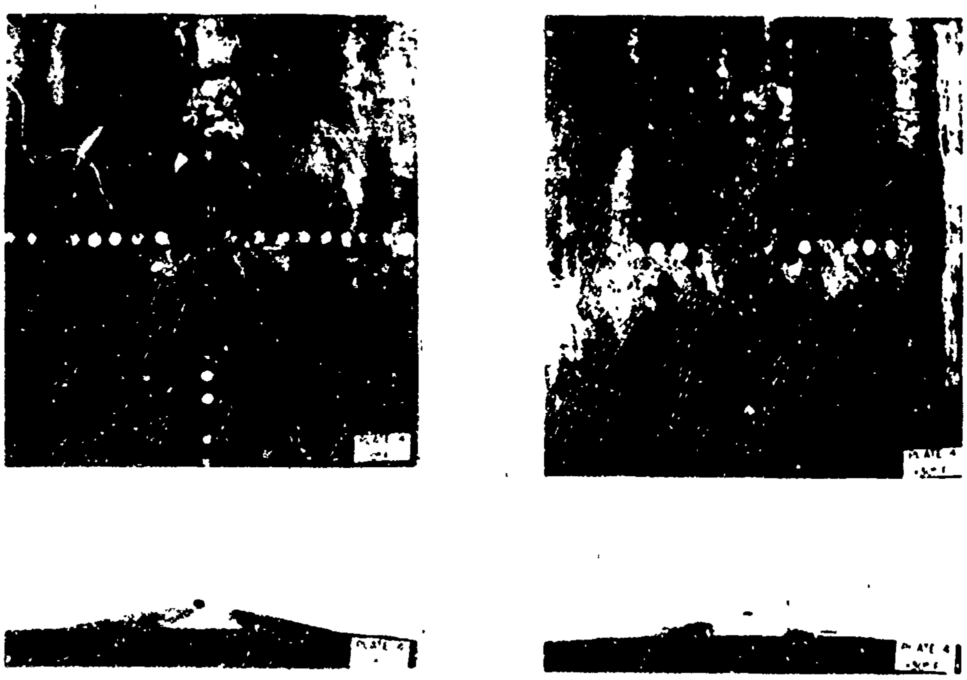

Fig. A-4. Explosion Bulge Plates from SMAW-30Kj Weldment

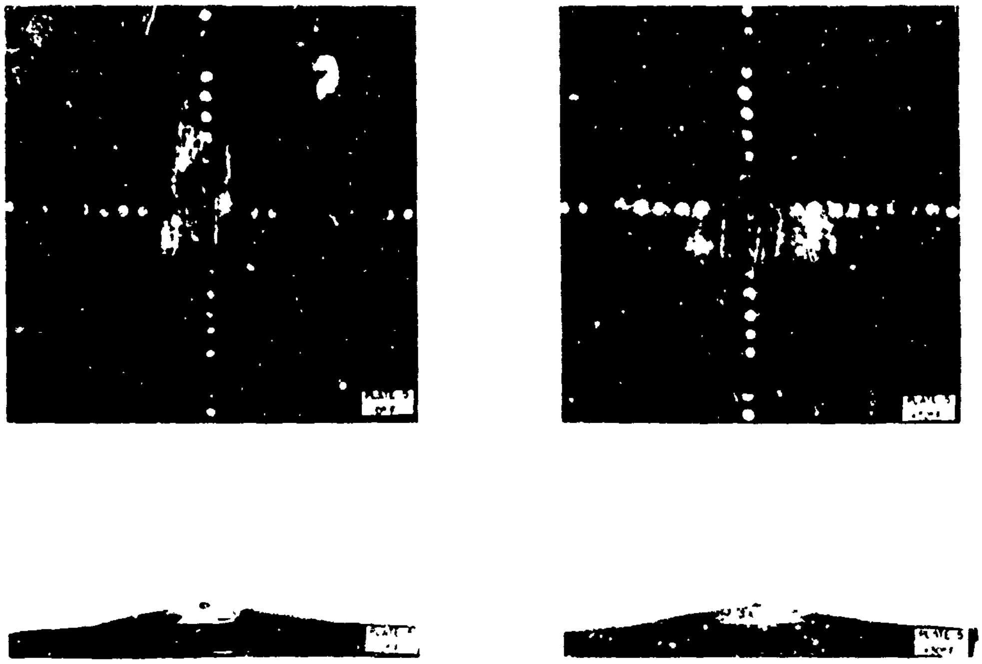

Fig. A-5. Explosion Bulge Plates from SMAW-50Kj Weldment

APPENDIX B

DETAILED WELDING PROCEDURE REPRESENTATIVE OF SHIPYARD PRACTICE

Specification No.: SwRI 07-2147-WP-2

Date: May 7, 1968

Scope: This specification is for the joining of A517 material to itself. This procedure is one of a series of three sub-arc procedures to be used for a specific program and simulates a procedure which has been used in actual merchant ship construction.

Base Material: ASTM 517-D was used for the procedure qualification.

Filler Metal and Flux: Armco W-25 wire 1/8 and 5/32 in., Linde 709-5 flux seal welding prior to automatic sub-arc E-8018-C3 1/8 inch.

Preheat and Interpass Temperature: Butt welds up to 1 1/2 in. shall have a preheat of 200°F minimum and maximum interpass temperature of 300°F. The maximum heat input shall be 65,000 J/inch.

Process and Electrical Characteristic: Automatic sub-arc - DC reverse polarity: Manual shield arc - (Seal weld) DC reverse polarity.

Joint Design: The design shall be as shown below.

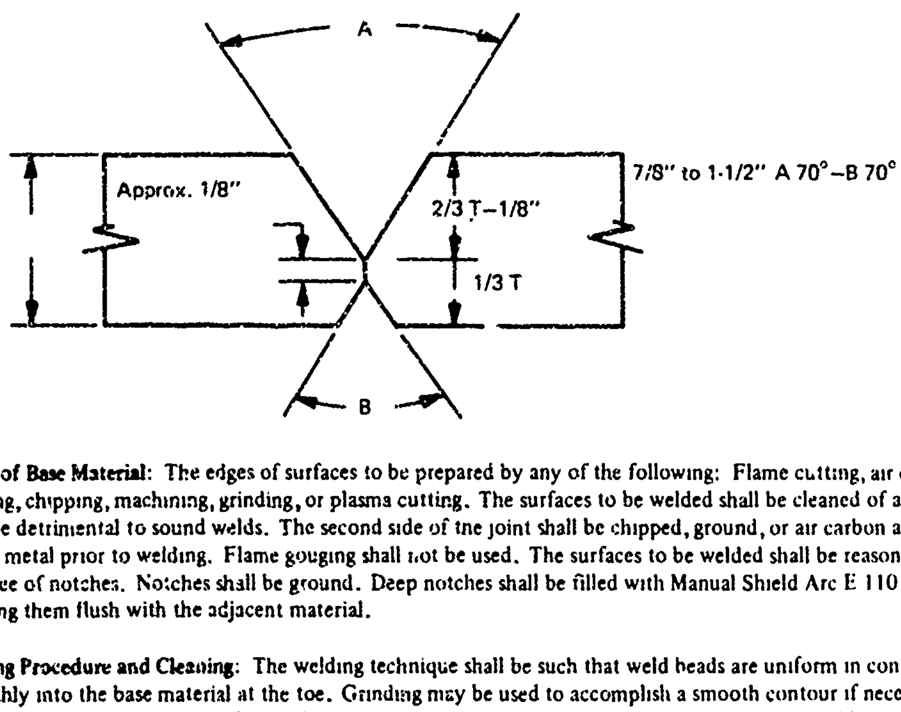

Preparation of Base Material: The edges of surfaces to be prepared by any of the following: Flame cutting, air carbon arc gouging, chipping, machining, grinding, or plasma cutting. The surfaces to be welded shall be cleaned of any matter that may be detrimental to sound welds. The second side of the joint shall be chipped, ground, or air carbon arc gouged to sound metal prior to welding. Flame gouging shall not be used. The surfaces to be welded shall be reasonably smooth and free of notches. Notches shall be ground. Deep notches shall be filled with Manual Shield Arc E 11018-M after grinding them flush with the adjacent material.

Joint Welding Procedure and Cleaning: The welding technique shall be such that weld beads are uniform in contour and taper smoothly into the base material at the toe. Grinding may be used to accomplish a smooth contour if necessary. All slag or flux remaining or any bead of weld shall be removed prior to depositing the next successive weld bead.

Arc strikes shall be avoided insofar as possible, care must be taken to strike arcs in the weld groove or in the way of the weld so they will be incorporated in the welds.

Defects Any cracks or blow holes that appear on the surface of any weld shall be removed by chipping, grinding, or air carbon arc gouging before depositing the next successive weld bead. Broken or cracked tacks shall be removed prior to seal welding.

Welding Position: Flat ±15°

Welding Repair: Welding may be repaired with Manual Shielded Arc Process.

Tempering Beads: Tempering welds shall be made so a new heat-affected zone *will not* be created. The temper bead toe should land approximately 1/8 in. from the base material (see sketch "Tempering Bead Technique").

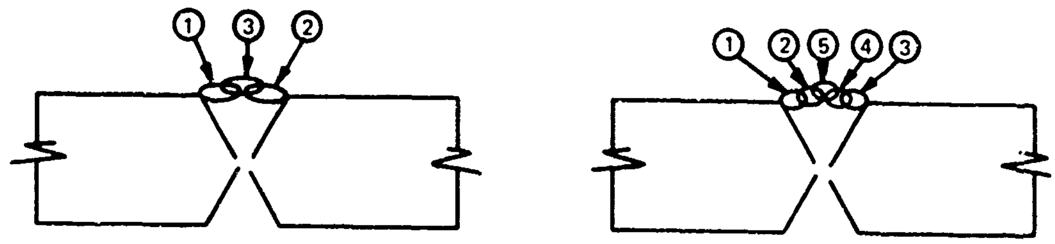

Tacking: For sub-arc welding, tacks shall be made using E 8018-C3 electrodes. These tacks shall be made so they can be incorporated in the seal weld.

Interpretation of Heat Cycle: Preheat temperature shall be maintained until the weld is complete or welds have been deposited equal to /3 of the wall thickness. Lower temperatures gradually until they are the ambient temperature.

Welding Procedure

1-1/4-in. plating shall be welded using the following procedure:
450 to 500 A, 30 V, 15 to 20 ipm, 1/8 in. + 5/32 in.
Armco W-25 filler metal, Linde 709-5 flux
200°F preheat, 300°F maximum interpass temperature
Heat Input, 40,000 to 60,000 J/inch.

APPENDIX C

WIDE-PLATE TEST DATA

Table C-1. Strain Gage Data on Wide-Plate Tests

Test No.	Specimen No.	Notch Type	Notch Length (in.)	Test Temp (°F)	Avg Strain (μin./in.) Gross Section	Avg Strain (μin./in.) Net Section
I	1	A	9.0	32	L-530[a]	L-600[a]
II	2	B	9.0	32	L-1000[b]	L-1350[b]
III	2	B	9.0	32	L-1590[a]	L-2125[a]
1	2	B	13.2	32	L-980[c]	N/A[d]
2	1	A	12.6	32	L-1280[c]	N/A[e]
3	3	A	8.8	32	L-930[f]	N/A[f]
4	3	A	11.2	32	L-980[c]	N/A[d]
5	WP[g]	A	8.8	32	L-1750[a]	L-1960[a]
6	WP[h]	A	8.8	32	L-1400[f]	L-1550[f]
7	WP[h]	A	24.0	32	L-1750[c]	L-2500[c]
8	4	A	8.0	32	L-1630[f]	L-2250[f]
					T-700[f]	T-450[f]
9	5[g]	A	8.3	32	L-2120[a]	L-2590[a]
					T-735[a]	T-
10	5[h]	A	8.3	32	L-1875[c]	L-2470[c]
					T-610[c]	T- -
11	6	A	8.5	0	L-1560[c]	-
12	7	A	8.5	-50	L-1190[c]	
13	8	A	8.5	0	L-1490[c]	-
14	9	A	8.5	0	L-925[c]	
15	10	A	8.5	50	L-1050[c]	-

(a)Machine out of stroke - test discontinued.
(b)Grip-to-specimen weld failed test discontinued.
(c)Fast fracture.
(d)Side grooved for full width of specimen.
(e)Side grooved 2 in. on each side of notch.
(f)Pop-in.
(g)With stiffeners.
(h)Stiffeners cut.

APPENDIX D

SLOW-BEND LOAD-DISPLACEMENT CURVES

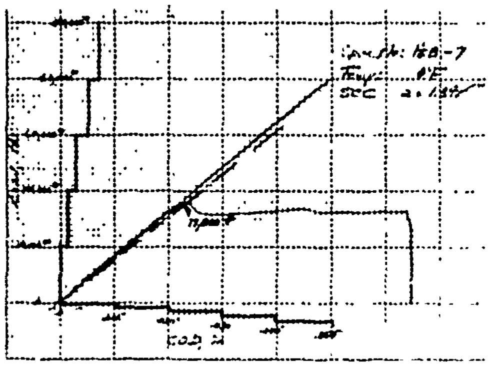

Fig. D-1.

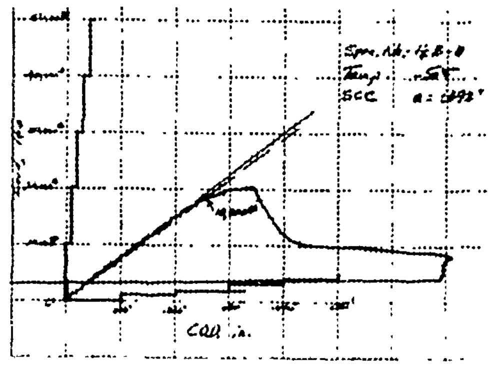

Fig. D-2.

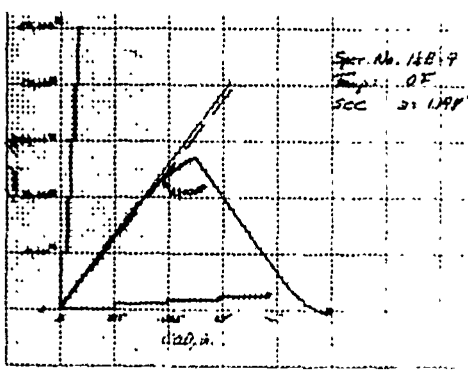

Fig. D-3.

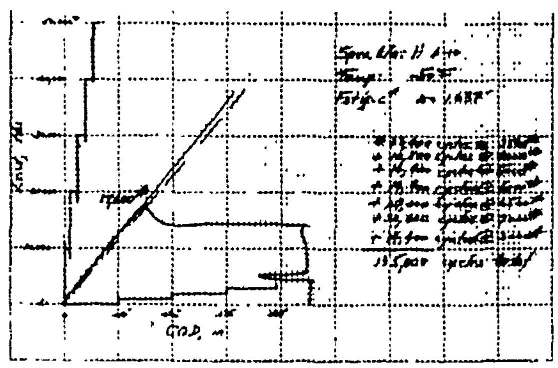

Fig. D-4.

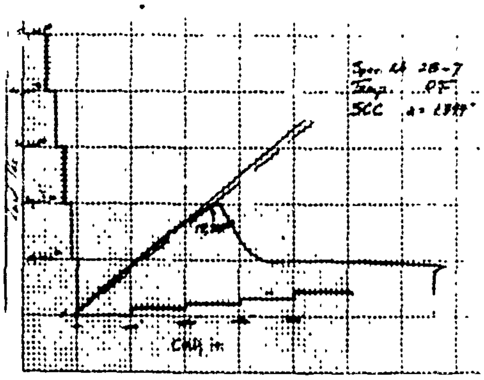

Fig. D-5.

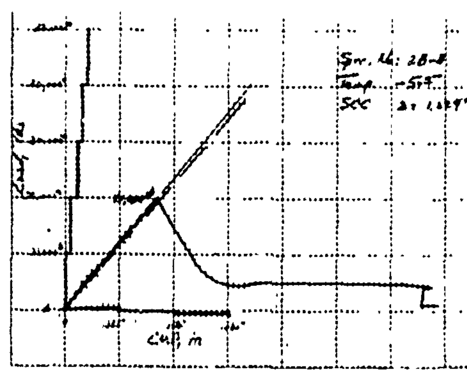

Fig. D-6.

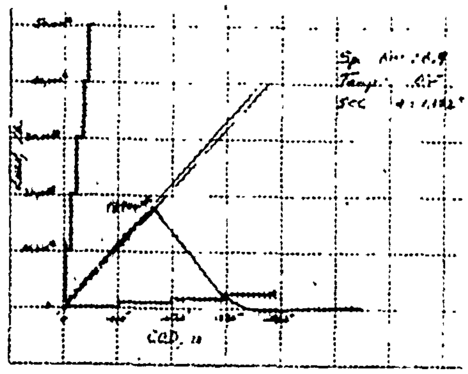

Fig. D-7.

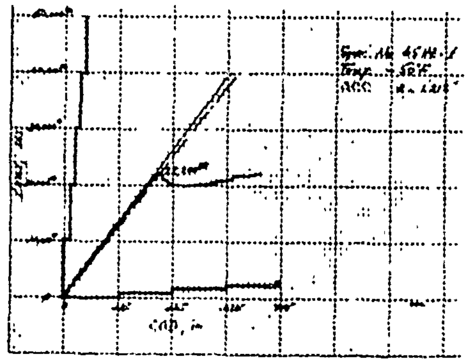

Fig. D-8.

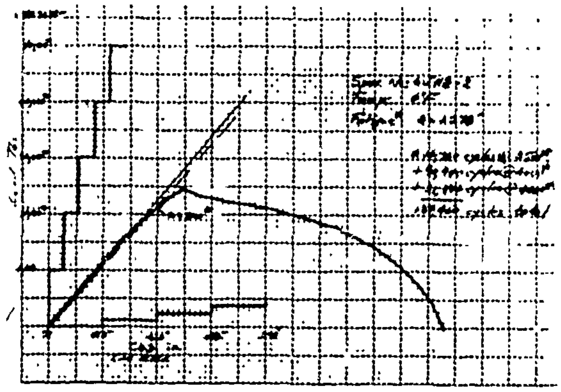

Fig. D-9.

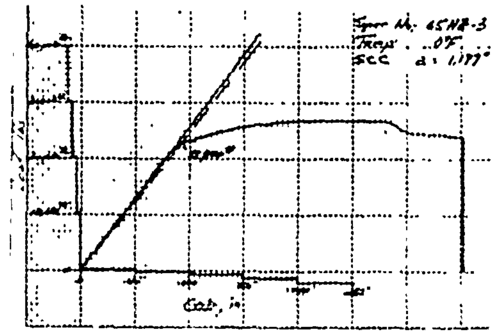

Fig. D-10.

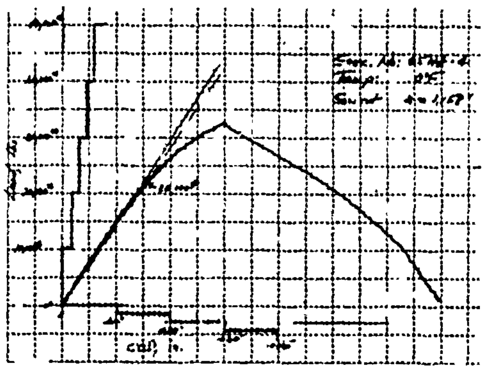

Fig. D-11.

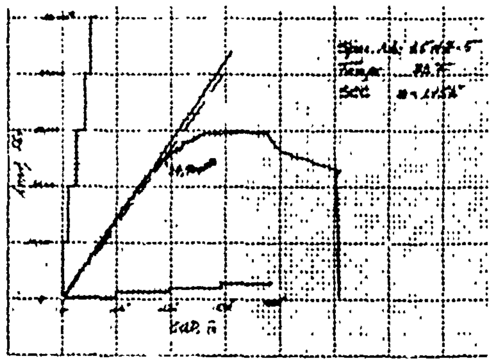

Fig. D-12.

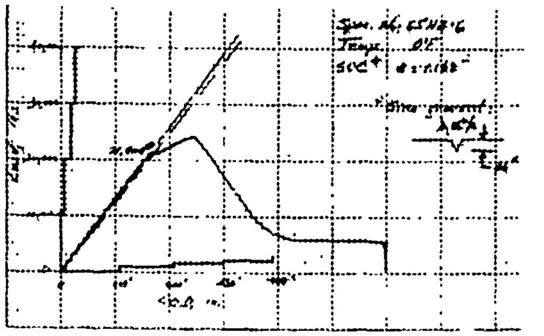

Fig. D-13.

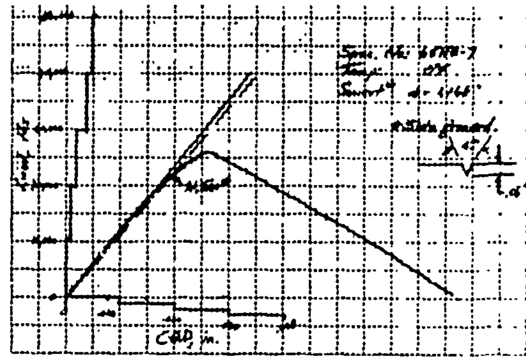

Fig. D-14.

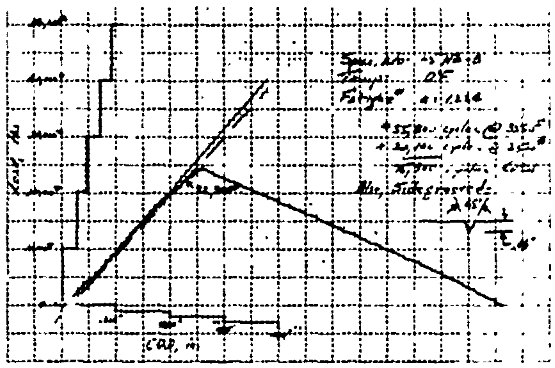

Fig. D-15.

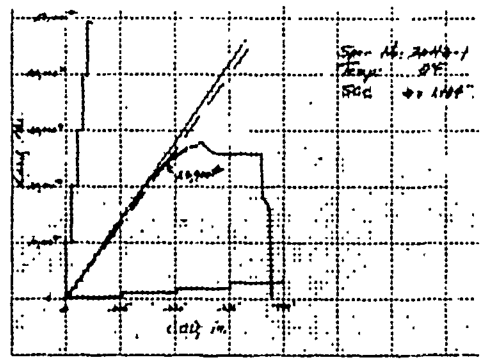

Fig. D-16.

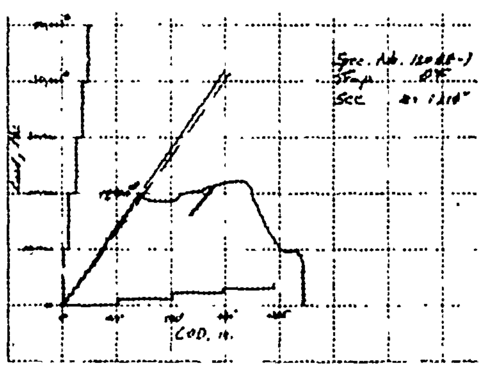

Fig. D-17.

APPENDIX E

NOTCHED IMPACT TEST DATA

Table E-1. Notched Impact Results on 1-¼-in. A517D Plate--Heat No. 46538

Specimen No.	Temp (°F)	Energy (ft-lb)	Fracture Appearance (% Shear)
1-1/4B-1	0	721	33
-2	+40	1329	60
-3	+80	1296	60
-4	+120	1427	67
-5	−40	596	27
-6	+180	1656	87

Table E-2. Notched Impact Results on 2-in. Plate A517D--Heat No. 46538

Specimen No.	Temp (°F)	Energy (ft-lb)	Fracture Appearance (% Shear)
2B-1	0	322	33
-2	+40	292	60
-3	+80	784	60
-4	+120	1038	67
-5	+180	1460	27
-6	+150	1362	87

SHIP RESEARCH COMMITTEE
Maritime Transportation Research Board
National Academy of Sciences-National Research Council

The Ship Research Committee has technical cognizance of the interagency Ship Structure Committee's research program:

PROF. R. A. YAGLE, Chairman, *Prof. of Naval Architecture, Univ. of Michigan*

DR. H. N. ABRAMSON, *Director, Dept. of Mechanical Sciences, Southwest Res. Inst.*

MR. W. H. BUCKELY, *Coordinator of Hydrojoil Struc. Res., Naval Ship R & D Center*

MR. E. L. CRISCUOLO, *Senior Nondestructive Testing Specialist, Naval Ordnance Lab.*

DR. W. D. DOTY, *Research Consultant, U. S. Steel Corporation*

PROF. J. E. GOLDBERG, *School of Civil Engineering, Purdue University*

PROF. W. J. HALL, *Prof. of Civil Engineering, University of Illinois*

MR. J. E. HERZ, *Chief Struc. Design Engineer, Sun Shipbuilding & Dry Dock Co.*

MR. G. E. KAMPSCHAEFER, JR., *Manager, Application Engineering, ARMCO Steel Corp.*

MR. R. C. STRASSER, *Director of Research, Newport News Shipbuilding & Dry Dock Co.*

CAPT R. M. WHITE, USCG, *Chief, Applied Engineering Section, U.S. Coast Guard Academy*

MR. R. W. RUMKE, *Executive Secretary, Ship Research Committee*

Advisory Group III, "Materials, Fabrication, and Inspection" prepared the project prospectus and evaluated the proposals for this project.

PROF. W. J. HALL, Chairman, *Prof. of Civil Engineering, University of Illinois*

MR. E. L. CRISCUOLO, *Sen. Nondestructive Testing Spec., Naval Ordnance Lab.*

DR. W. D. DOTY, *Research Consultant, U. S. Steel Corporation*

MR. P. E. JAQUITH, *Planning Supervisor, Bath Iron Works Corporation*

MR. G. E. KAMPSCHAEFER, JR., *Manager, Application Engr., ARMCO Steel Corporation*

PROF. A. W. PENSE, *Prof. of Metallurgy, Lehigh University*

DR. S. YUKAWA, *Consulting Engr., General Electric Company*

The SR-177 Project Advisory Committee provided the liaison technical guidance, and reviewed the project reports with the investigator.

MR. G. E. KAMPSCHAEFER, JR., Chairman, *Manager, Application Engr., ARMCO Steel Corp.*

DR. D. P. CLAUSING, *Sen. Scientist, Edgar C. Bain Lab. for Fund. Res., U.S. Steel Corp.*

PROF. S. T. ROLFE, *Civil Engr. Dept., University of Kansas*

SHIP STRUCTURE COMMITTEE PUBLICATIONS

These documents are distributed by the National Technical Information Service, Springfield, Va. 22151. These documents have been announced in the Clearinghouse Journal U.S. Government Research & Development Reports (USGRDR) under the indicated AD numbers.

SSC-219, *Crack Propagation and Arrest in Ship and Other Steels* by G. T. Hahn, R. G. Hoagland, P. N. Mincer, A. R. Rosenfield, and M. Sarrate. 1971.

SSC-220, *A Limited Survey of Ship Structural Damage* by S. Hawkins, G. H. Levine, and R. Taggart. 1971.

SSC-221, *Response of the Delta Test to Specimen Variables* by L. J. McGeady. 1971.

SSC-222, *Catamarans - Technological Limits to Size and Appraisal of Structural Design Information and Procedures* by N. M. Maniar and W. P. Chiang. 1971.

SSC-223, *Compressive Strength of Ship Hull Girders - Part II - Stiffened Plates* by H. Becker, A. Colao, R. Goldman, and J. Pozerycki. 1971.

SSC-224, *Feasibility Study of Glass Reinforced Plastic Cargo Ship* by R. J. Scott and J. H. Sommella. 1971.

SSC-225, *Structural Analysis of Longitudinally Framed Ships* by R. Nielson, P. Y. Chang, and L. C. Deschamps. 1972.

SSC-226, *Tanker Longitudinal Strength Analysis - User's Manual and Computer Program* by R. Nielson, P. Y. Chang, and L. C. Deschamps. 1972.

SSC-227, *Tanker Transverse Strength Analysis - User's Manual* by R. Nielson, P. Y. Chang, and L. C. Deschamps. 1972.

SSC-228, *Tanker Transverse Strength Analysis - Programmer's Manual* by R. Nielson, P. Y. Chang, and L. C. Deschamps. 1972.

SSC-229, *Evaluation and Verification of Computer Calculations of Wave-Induced Ship Structural Loads* by P. Kaplan and A. I. Raff. 1972.

SSC-230, *Program SCORES -- Ship Structural Response in Waves* by A. I. Raff. 1972.

SSC-231, *Further Studies of Computer Simulation of Slamming and Other Wave-Induced Vibratory Structural Loadings on Ships in Waves* by P. Kaplan and T. P. Sargent. 1972.